Available online at www.sciencedirect.com
SCIENCE DIRECT
Sensors and Actuators A 111 (2004) 44–50
SENSORS AND ACTUATORS A PHYSICAL
www.elsevier.com/locate/sna

Surface micromachined glass and polysilicon microchannels using MUMPs for BioMEMS applications☆

Ki Bang Lee*, Liwei Lin

Berkeley Sensor and Actuator Center, Department of Mechanical Engineering, University of California at Berkeley, 1113 Etcheverry Hall, Berkeley, CA 94720-1740, USA

Received 27 June 2003

Abstract

MUMPs (Multi-User MEMS Process) based microchannels made of either glass or polysilicon have been successfully designed, fabricated and tested. The fabrication process used timed wet-chemical etching to selectively etch sacrificial materials with the assistance of etch holes. The prototype glass and polysilicon microchannels have cross-section areas of 70 μm × 4 μm and 70 μm × 2 μm, respectively, and both microchannels have been tested to transport and contain water by means of surface tension. A simplified surface tension analysis shows that the height of the etch holes and the surface tension of the working liquid inside the microchannel dominates the pressure difference that holds the liquid from leaking outside the microchannel via etch holes. Because these microchannels are fabricated using the foundry-based micromachining process, they present opportunities for economical prototyping and have great potential for integration with other microfluidic devices for system-level applications, such as DNA chip and lab-on-a-chip.
© 2003 Elsevier B.V. All rights reserved.

Keywords: Microchannel; Microfluidics; BioMEMS; Surface tension; MEMS; Microsystem; Micromachine

1. Introduction

Microfluidic systems in combination with medical, electrical, chemical, and DNA technologies are promising to improve medical instruments, such as DNA chips [1] and lab-on-a-chip [2]. Microchannels are essential in these systems to carry liquid samples from one position to another and to protect sensitive micro reactions from contaminations by exposing to the environment. The majority of microfluidic devices use bulk-micromachining technologies [3,4] to etch microchannels into substrates and wafer bonding processes, such as anodic bonding or fusion bonding, to seal and complete the top surface. As a result, the material cost is increased because one extra wafer is needed as the cap to encapsulate microfluidic systems. In contrast, several surface-micromachined channels [5,6] have been developed for microfluidics devices such as microneedles [5] and they are interesting alternative solutions to construct microchannels.

The standard surface-micromachining process, MUMPs (Multi-User MEMS Process) [7], has been widely used in the MEMS community, including universities, industry and research labs all over the world, to make polysilicon-based, moveable microstructures [8], such as mirrors [9], or even power sources [10,11]. In this paper, MUMPs based, surface micromachined glass and polysilicon microchannels are designed, fabricated and tested. These microchannels have the potential to be integrated with other micromachined microfluidic systems, including DNA chip and lab-on-a-chip. As such, a new class of future applications in microfluidics that has not been conceived previously may be envisioned based on these foundry-based microchannels.

2. Microchannels

Fig. 1(a) and (b) show the schematic diagram of the surface-micromachined glass and polysilicon microchannels on a substrate. These surface-micromachined channels are designed to have hydrophilic interiors in order to carry water-based working liquids internally. In the case of polysilicon microchannel of Fig. 1(b), hydrophilic surface is formed due to the native silicon dioxide layer grown on top of the polysilicon surface. The placements of etch holes in

☆ A portion of this paper was presented at the 16th IEEE Micro Electro Mechanical Systems Conference, Kyoto, January 19–23, 2003.

* Corresponding author. Tel.: +1-510-642-8983; fax: +1-510-642-6163.
E-mail address: kblee@me.berkeley.edu (K.B. Lee).

0924-4247/$ – see front matter © 2003 Elsevier B.V. All rights reserved.
doi:10.1016/j.sna.2003.10.027

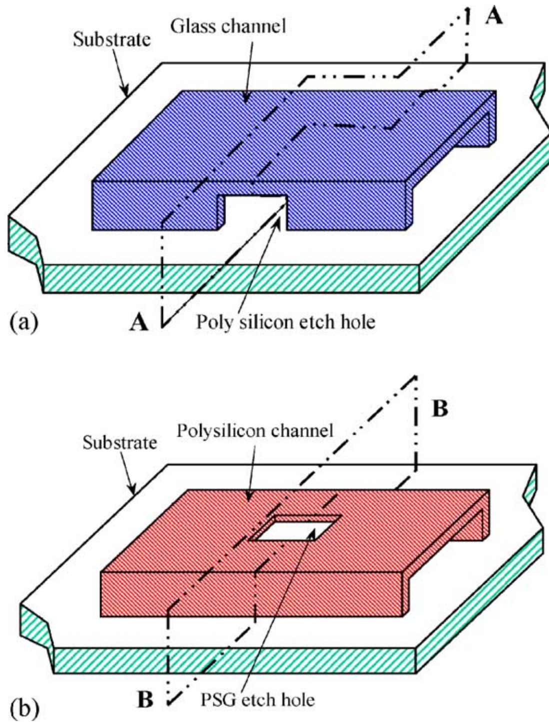

Fig. 1. Schematic diagram of surface-micromachined channels based on (a) glass and (b) polysilicon caps. The fabrication processes illustrating the cross section areas A-A and B-B are described in Figs. 2 and 3, respectively.

Fig. 1(a) and (b) are on the sidewall for the glass microchannel and on the top cap for the polysilicon microchannel, respectively, in this paper. However, one can easily change the placement of etch holes based on the design principles derived in this work. These etch holes serve for two purposes: (1) as the etching paths to remove sacrificial layers inside the microchannels; and (2) as easy getaways for air bubbles that commonly clog microchannels during the microfluidic operations. These holes must be small such that surface tension of liquid can hold the working liquid inside the microchannel. The standard surface-micromachining process, MUMPs [7] with three polysilicon layers and two PSG layers, is used to fabricate the surface-micromachined glass and polysilicon microchannels such that they could be integrated together with other surface-micromachined devices.

Fig. 2 shows the microfabrication process of the glass channel using the cross-section, A-A, of Fig. 1(a) as the illustration purpose. Experimentally, the top caps of microchannels are made of PSG and the anchors that hold the top caps are made of polysilicon. In Fig. 2(a), a 2 μm thick PSG1 layer is deposited as the first sacrificial layer and patterned for polysilicon anchors. A 2 μm thick polysilicon layer (poly1) is deposited and patterned as the lower protective polysilicon layer to protect the structural cap glass (PSG2). After these steps, Fig. 2(b) applies. Afterwards, the 0.75 μm thick PSG2 layer is deposited and patterned as the top channel cap in Fig. 2(c), and a 1.5 μm thick poly2 layer is deposited and patterned as the upper protective layer to cover the PSG2 cap structure during the later release etching process.

The whole wafer is put into HF solution to remove the sacrificial PSG1 layer as shown in Fig. 2(e) while the PSG2 microchannel layer is protected by the upper (poly2) and lower (poly1) protective polysilicon layers. Afterwards, the protective poly1 and poly2 layers are removed in a timed, wet silicon etchant as shown in Fig. 2(f) to obtain glass microchannels. The timed etching process keeps part of the polysilicon anchor to remain on the substrate to support microchannels as illustrated in Fig. 2(f).

Fig. 3 shows the fabrication process of the polysilicon microchannels. In Fig. 3(a), the poly0 layer is deposited and patterned to get higher channel height. The PSG1 sacrificial layer is deposited and patterned for the microchannel body

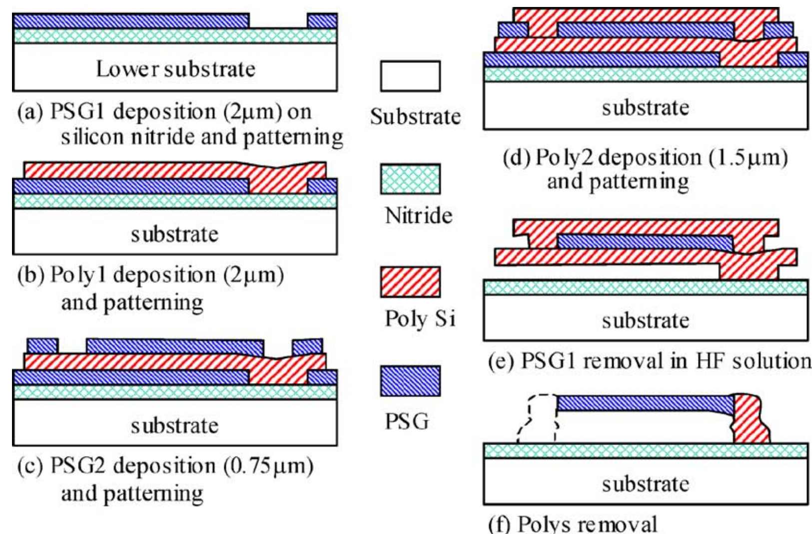

Fig. 2. Fabrication process for the glass microchannel: cross-section A-A in Fig. 1(a) is shown.

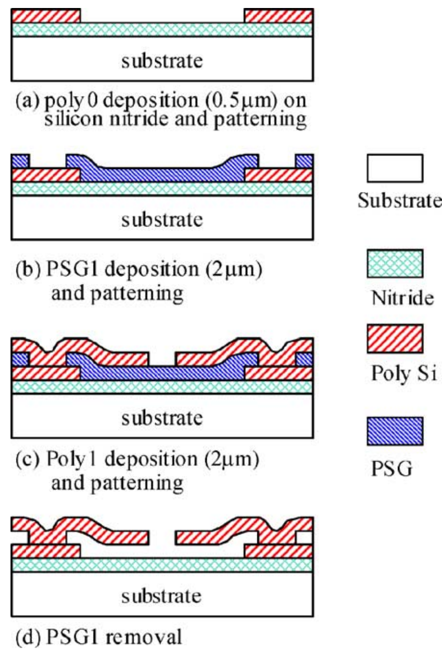

Fig. 3. Fabrication process for the silicon microchannel: cross-section B-B in Fig. 1(b) is shown.

as shown in Fig. 3(b). Afterwards, a 2 μm thick poly1 layer is deposited as the channel structure layer and patterned in Fig. 3(c). After removing the sacrificial PSG1 layer in HF solution via the etch holes on the top surface of the microchannel, the process is completed by rinsing and drying.

3. Results and discussions

Fig. 4 shows the SEM microphoto of the glass microchannel fabrication process of Fig. 2(e) after removing the PSG1 layer in the HF solution. The two upper and lower protective layers of polysilicon are still in tact to protect the second glass layer (PSG2) as the top layer of glass microchannel. Etch holes can be identified in this figure for the removal of sacrificial PSG1 layer under the lower protective polysilicon layer. The anchors, made of poly1 and poly2 layers, support a sandwich layer consisting of poly1, PSG2 and poly2.

Table 1
KOH etching solution

Temperature	80 °C
Stirring	600 rpm
Etch rate (for polysilicon)	1 μm/min

KOH:DI water is 1:2 (w/w).

The KOH solution as listed in Table 1 is used to remove the two upper and lower protective polysilicon layers as shown in Fig. 4. The temperature of KOH solution bath is set at a constant 80 °C and the bath is stirred at 600 rpm to improve the uniformity of the etching process. The etch rate is about 1 μm/min and the polysilicon layers are completely etched within 90 s. Fig. 5 shows the finished microstructure of a glass microchannel (PSG2) with a cross-section of 70 μm in width and 4 μm in height after the removal of the sacrificial polysilicon layers of poly1 and poly2. In Fig. 5, the glass channel made of PSG2 is supported by polysilicon anchors as shown in Fig. 2(f). It is noted that the stacked polysilicon anchors shown in Fig. 2(f) survived after the removal of the upper and lower protective polysilicon layers. It has also been observed that if the final releasing etching time period is too short, polysilicon residuals can be found on the PSG2 microchannel. On the other hand, if the etching time period is too long, the polysilicon anchors could disappear totally. Therefore, the release etching time is very critical and must be carefully controlled. For example, Fig. 6 shows the optical microphoto of a glass microchannel when the etching period is too short and some poly1 residuals can be clearly observed.

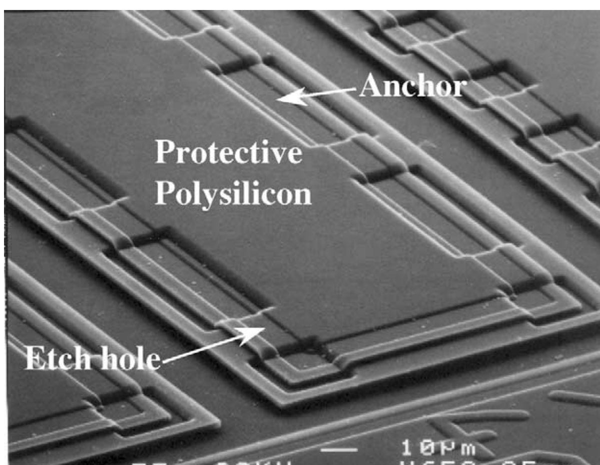

Fig. 4. A SEM microphoto showing the glass microchannel fabrication process at the end of Fig. 2(e) before the removal of protective polysilicon layers. Two protective polysilicon layers are still in tact to protect the second glass layer (PSG2) while the first glass layer (PSG1) is etched.

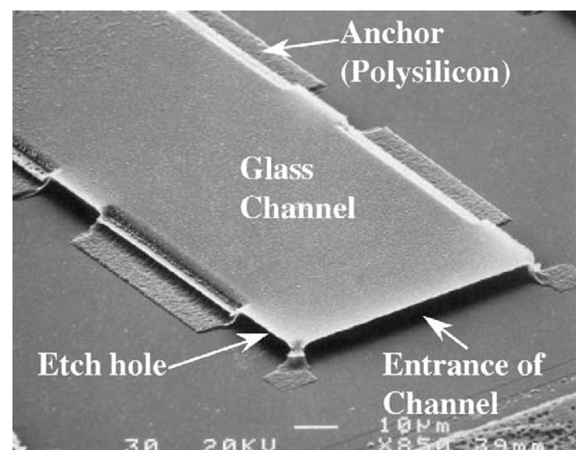

Fig. 5. A SEM microphoto showing a fabricated glass microchannel. The top glass (PSG2) layer is 0.75 mm thick. The cross-section of the microchannel is 70 μm wide and 4 μm high.

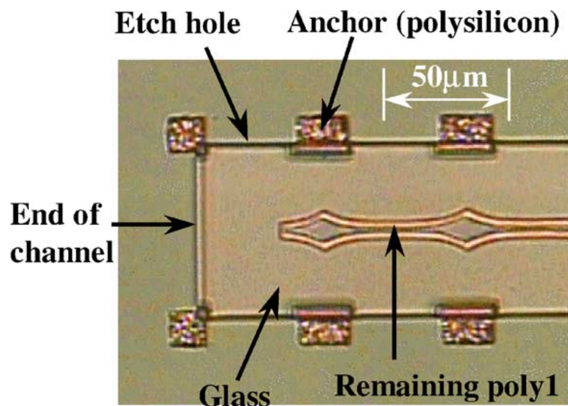

Fig. 6. Optical microphoto showing the glass microchannel when the polysilicon etching period is short of completion: some polysilicon (poly1) remains in the center of the glass microchannel.

Fig. 7 shows the optical microphoto of a complete glass microchannel after water is supplied from the designed reservoir entrance. Because glass is transparent, reactions inside microchannels may be observed but it is difficult to tell the differences between the clean water and the transparent microchannel with respect to the background substrate. It is also noted that surface tension force, due to hydrophilic surfaces of the top glass layer and the bottom silicon nitride layer, provides the preferable condition to allow water entering the microchannel. Fig. 8 is a close-up view of the marker "C" in Fig. 7 to examine further the area around the etch hole, which is 40 μm wide and 4 μm high in this case. Figs. 7 and 8 show that the surface tension of water plays two important roles at the same time: (1) to drive external water into the microchannel, and (2) to prevent water inside the microchannel from leaking out.

Figs. 9 and 10 provide some theoretical explanations of the surface tension effects. Fig. 9 is a schematic showing a simplified, one-dimensional model for the surface tension effect. The two driving forces come from the surface tension effect and may be represented as, $2\sigma b$, where σ is the surface tension and b is the width of the microchannel. From the simple diagram of Fig. 9(b), the governing equations of the water in the microchannel are obtained as follows [15]:

$$\text{Momentum eq.}: \quad \frac{\partial u}{\partial t} = -\frac{1}{\rho}\frac{\mathrm{d}p}{\mathrm{d}x} + \frac{\mu}{\rho}\frac{\partial^2 u}{\partial y^2} \tag{1}$$

$$\text{Pressure eq.}: \quad -\frac{\mathrm{d}p}{\mathrm{d}x} = \frac{2\sigma}{h\,L(t)}, \tag{2}$$

where ρ, u, p, x, y, μ, h, L, t and σ are the density of the water, the velocity of water, the pressure in the channel, the coordinates in the horizontal and vertical directions, the viscosity of water, the height of the channel, the displacement of the water meniscus, time, the surface tension as a driving force, respectively. b and τ are the channel width and the shear stress on the channel wall. It is noted in Eqs. (1) and (2) that the surface tension generates pressure and the water in the channel is transported by the pressure in the x direction while the viscous force drags the water. For $h \ll b$, $t \gg$ micro second, the displacement of the water meniscus is obtained as follows [15]:

$$L(t) = \sqrt{L_0^2 + \left(\frac{\sigma h}{2\mu}\right) t}, \tag{3}$$

where L_0 is the initial displacement at $t = 0$. From Eq. (3), the displacement, L, is proportional to square-root of time.

Fig. 10 illustrates the condition around the etch holes after filling up the microchannel. The liquid meniscus generated at the interface between water and external air provide a pressure difference to hold the water from leaking and the magnitude of the pressure caused by surface tension can be expressed as follows [12]:

$$p = 2\sigma\left(\frac{1}{h} + \frac{1}{w}\right), \tag{4}$$

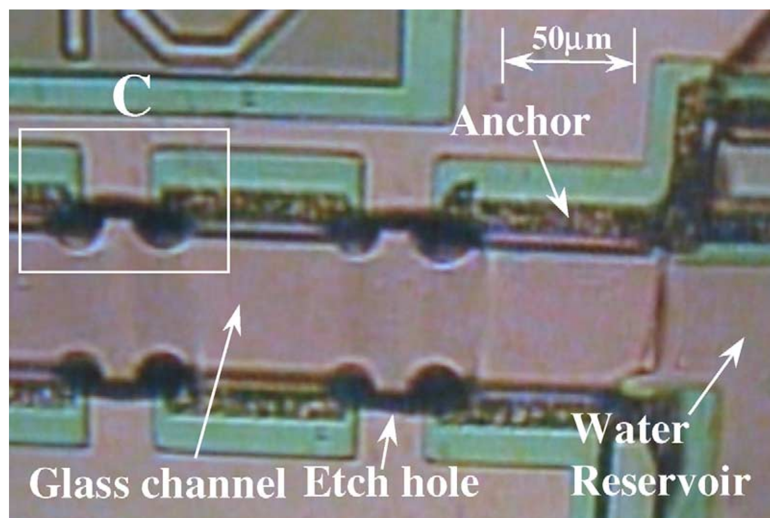

Fig. 7. An optical microphoto of the glass microchannel showing that water is transported by surface tension after a droplet of water is placed on the water reservoir.

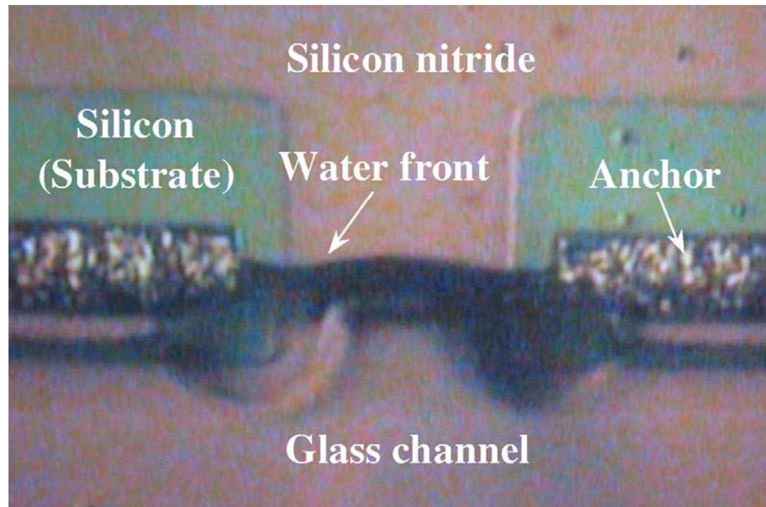

Fig. 8. Close-up view of marker "C" in Fig. 7 showing that water front is formed around the etch hole and surface tension prevents the leaking of water.

where σ, h and w are the surface tension of the working liquid, the channel height and the width of the etch hole, respectively. For $h \ll w$, Eq. (4) is simplified to $p = 2\sigma/h$. Therefore, the pressure difference strongly depends on the surface tension of working liquid and the channel height. It implies that the width of the etch hole plays a secondary role in holding the working liquid as long as the dimension of width is much larger than the thickness. The calculated pressure difference caused by surface tension is $p = 7.36\times10^{-6}(1/4\times10^{-6}+1/70\times10^{-6}) = 1.9\times10^{4}$ Pa in the case of Fig. 8 ($h = 4\,\mu$m, $w = 70\,\mu$m, $\sigma = 7.36\times10^{-2}$ N/m for water at 20 °C). Fig. 11 shows the optical microphoto showing a possible extension of using the glass microchannel to bioMEMS applications. In this case, a droplet of blood is placed in the right entrance of the channel. Ultraviolet or visible light detector can be used to detect biochemical reaction through the transparent glass channel.

Fig. 12 shows the SEM microphoto of a fabricated polysilicon microchannel with etch holes of $20\,\mu\text{m} \times 20\,\mu\text{m}$ on the top cap. The cross-section of the microchannel is

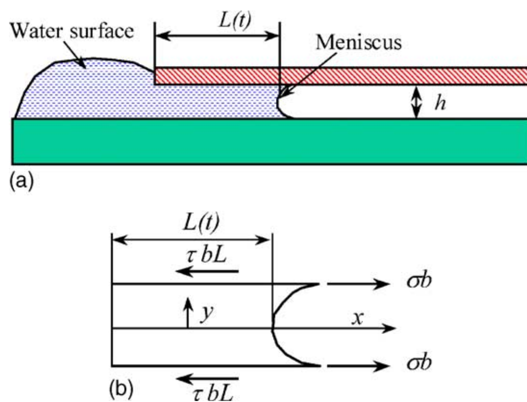

Fig. 9. Schematic for showing surface tension driving: surface tension drives water into the channel while viscous forces drag the water. (a) two-dimension model, (b) forces on the water in the channel.

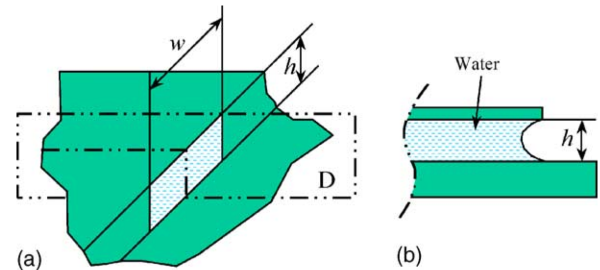

Fig. 10. Surface tension around the etch hole: (a) etch hole after applying water, (b) cross section of plane D of (a); the meniscus is generated due to surface tension of liquid/air interface.

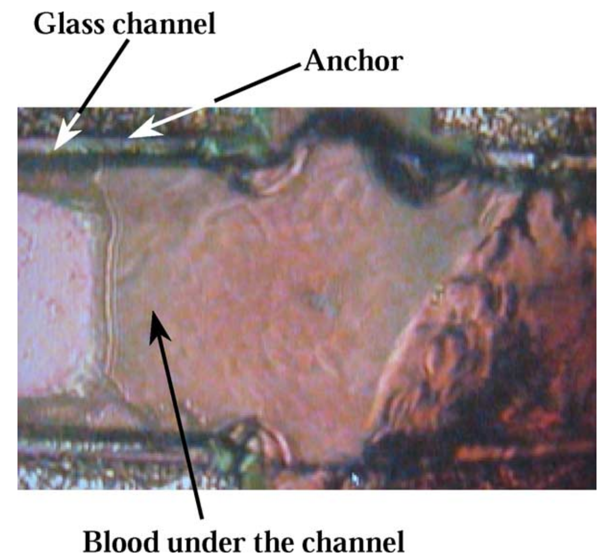

Fig. 11. Optical microphoto showing blood is flowing under the transparent glass microchannel after a droplet of blood is placed in front of the entrance of the channel.

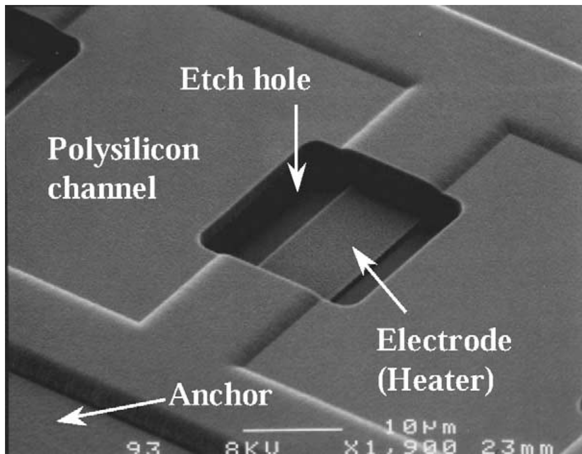

Fig. 12. A SEM microphoto showing a fabricated polysilicon microchannel: Electrodes (heater) made of poly0 are laid for possible sensing or actuation applications.

70 μm wide and 2 μm high. A microelectrode (heater) made of polysilicon (poly0) is laid as shown for further sensing and actuation applications in microfluidic systems. Based on Eq. (4), the pressure generated by surface tension of water will be 3.8×10^4 Pa. Fig. 13 shows an optical microphoto after water is applied to a polysilicon microchannel. It is found that surface tension force due to hydrophilic native oxide on the polysilicon surface of the microchannel, assists the water to flow inside the microchannel and prevents water from leaking out. On possible feature to transfer working liquid in these surface-micromachined microchannels is to assure that the applied pumping pressure is less than 5×10^3 Pa [13,14] to prevent leakage through the etch holes. Moreover, although only two types of MUMPs-based, surface-micromachined microchannels are presented in this work, there are many other possible designs and procedures that one may apply to the MUMPs process to make surface-micromachined microchannels. Alternatively, one can easily fabricate other types of microchannels without following MUMPs either by bulk- or surface-micromachining processes in clean room.

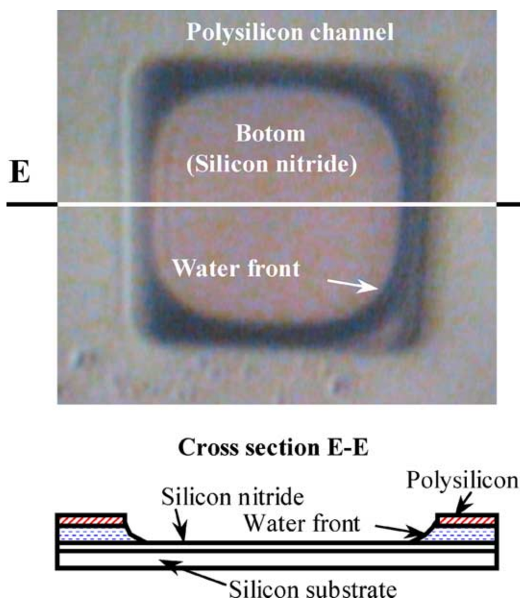

Fig. 13. Optical microphoto showing the water front: surface tension force due to hydrophilic native oxide on top of the polysilicon channel assists the water to flow inside the channel.

4. Conclusions

MUMPs (Multi-User MEMS Process) based microchannels made of glass or have been successfully designed, fabricated and tested. The fabrication process utilized the design rules set by the foundry service and used timed release etching processes to selectively etch sacrificial layers with the assistance of etch holes. As a result, either glass or polysilicon microchannels can be fabricated. The prototype glass microchannel has a cross section of 70 μm × 4 μm and the polysilicon microchannel has a cross section of 70 μm × 2 μm. A simplified surface tension analysis shows that the height of the etch holes and the surface tension of the working liquid inside the microchannel determines the pressure difference that holds the liquid from leaking outside the microchannel via the etch holes. These microchannels have the potential to be integrated with other micromachined microfluidic systems for device applications, including DNA chip and lab-on-a-chip.

Acknowledgements

This project is supported in part by a DARPA/DSO/Bio-Flips grant (F30602-00-2-0566).

References

[1] K. Takahashii, K. Seio, M. Sekine, O. Hino, M. Esashi, A photochemical/chemical direct method of synthesizing high-performance deoxyribonucleic acid chips for rapid and parallel gene analysis, Sens. Actuators B 38 (2002) 67–76.

[2] R.-L. Chien, J.W. Parce, Multiport flow-control system for lab-on-a-chip microfluidic devices, Fresenius J. Anal. Chem. 371 (2) (2001) 106–111.

[3] M. Lee, M. Wong, Y. Zohar, Design, Fabrication and characterization of an integrated micro heat pipe, in: Proceeding of the Fifteenth IEEE International Conference on Micro Electro Mechanical Systems, Las Vegas, Nevada, USA, January 20–24, 2002, pp. 85–88.

[4] M.J. DeBar, D. Liepmann, Fabrication and performance testing of a steady thermocapillary pump with no moving parts, in: Proceeding of the Fifteenth IEEE International Conference on Micro Electro Mechanical Systems, Las Vegas, Nevada, USA, January 20–24, 2002, pp. 109–112.

[5] L. Lin, A.P. Pisano, Silicon-processed microneedles, IEEE J. Microelectro-Mech. Systems 8 (1) (1999) 78–84.

[6] D. Bhusari, H.A. Reed, M. Wedlake, A.M. Padovani, S.A.B. Allen, P.A. Kohl, Fabrication of air-channel structures for microfluidic,

microelectromechanical, and micro-electronic applications, IEEE J. Microelectro-Mech. Systems 10 (3) (2001) 400–408.
[7] D.A. Koester, R. Mahadevan, B. Hardy, K.W. Markus, MUMPs Design Handbook, Revision 6.0, Cronos Integrated Microsystems, A JDS Uniphase Company, 2001.
[8] W.C. Tang, T.-C.H. Nguyen, R.T. Howe, Laterally driven polysilicon resonant microstructures, Sens. Actuators A 20 (1989) 25–32.
[9] J.T. Nee, R.A. Conant, R.S. Muller, K.Y. Lau, Lightweight, optically flat micromirrors for fast beam steering, 2000 IEEE/LEOS International Conference on Optical MEMS, Piscataway, NJ, USA, 2000, pp. 9–10.
[10] K.B. Lee, L. Lin, Electrolyte based on-demand and disposable microbattery, in: Proceeding of the Fifteenth IEEE International Conference on Micro Electro Mechanical Systems, Las Vegas, Nevada, USA, January 20–24, 2002, pp. 236–239.
[11] K.B. Lee, F. Sammoura, L. Lin, Water activated disposable and long shelf life microbatteries, in: 16th IEEE International Conference on Micro Electro Mechanical System, MEMS 2003, Kyoto, Japan, January 19–23, 2003, pp. 387–390.
[12] F.M. White, Fluid Mechanics, second ed., McGraw-Hill, New York, 1986.
[13] S. Santra, P. Holloway, C.D. Batich, Fabrication and testing of a magnetically actuated micropump, Sens. Actuators B 87 (2002) 358–364.
[14] J.-H. Tsai, L. Lin, A thermal-bubble-actuated micronozzle-diffuser pump, J. Microelectromech. Systems 11 (6) (2002) 665–671.
[15] L.-J. Yang, T.-J. Yao, Y.-L. Huang, Y. Xu, Y.-C. Tai, Marching velocity of capillary meniscuses in microchannels, in: Proceeding of the Fifteenth IEEE International Conference on Micro Electro Mechanical Systems, Las Vegas, Nevada, USA, January 20–24, 2002, pp. 93–96.

Biographies

Ki Bang Lee was born in Korea, in 1962. He received his BS, MS, and PhD degrees, all in mechanical engineering, from the Hanyang University, Seoul, Korea, and the Korea Advanced Institute of Science and Technology (KAIST), Korea, in 1985, 1987, and 2000, respectively. He worked with Samsung Advanced Institute of Technology (SAIT), Yonginsi, Korea, during 1987–2000. With Samsung and KAIST, he worked on the projects on design and fabrication of micromirror and microactuator for data storage system and hard disk drive, microactuators for tuning frequency and quality factors, design and fabrication of microgyroscope, color printer and inkjet print head, simulation and measurement of air gap between the magnetic head and tape of VCR (Video Cassette Recorder), and noise and vibration control for refrigerators. He has been a post-doctoral researcher of the Berkeley Sensors and Actuator Center (BSAC) at the University of California at Berkeley since November 2000. Since joining BSAC, he has been involved in the projects of Massively Parallel Post-Packaging for MEMS, Integrated Microwatt Transceivers and Water-powered Bioassay Systems that are all supported by Defense Advanced Research Projects Agency (DARPA). His research interests include MEMS (Microelectromechanical Systems); bioMEMS; micropower generation including disposable microbattery; design and fabrication of microsensors and microactuators; integrated disposable microsystems such as DNA chips, diagnostic devices, and/or labs-on-a-chip with disposable micropower; microvehicles for MEMS/bioMEMS application; microfluidic devices.

Liwei Lin (S'92–M'93) received the MS and PhD degrees in mechanical engineering from the University of California, Berkeley, in 1991 and 1993, respectively. From 1993 to 1994, he was with BEI Electronics, Inc., USA, in research and development of microsensors. From 1994 to 1996, he was an Associate Professor in the Institute of Applied Mechanics, National Taiwan University, Taiwan. From 1996 to 1999, he was an Assistant Professor at the Mechanical Engineering and Applied Mechanics Department at the University of Michigan, Ann Arbor. In 1999, he joined the University of California at Berkeley and is now an Associate Professor at Mechanical Engineering Department and Co-Director at Berkeley Sensor and Actuator Center, NSF/Industry/University research cooperative center. His research interests are in design, modeling, and fabrication of microstructures, microsensors, and microactuators as well as mechanical issues in microelectromechanical systems including heat transfer, solid/fluid mechanics, and dynamics. He holds eight US patents in the area of MEMS. Dr. Lin is the recipient of the 1998 NSF CAREER Award for research in MEMS Packaging and the 1999 ASME Journal of Heat Transfer Best Paper Award for his work on microscale bubble formation. He served as Chairman of the Micromechanical Systems Panel of the ASME Dynamic Systems and Control Division in 1997 and 1998 and led the effort in establishing the MEMS subdivision in ASME and is currently the Vice Chairman of the Executive Committee.